

NOTICE: this is the author's version of a work that was accepted for publication in Lithos. Changes resulting from the publishing process, such as peer review, editing, corrections, structural formatting, and other quality control mechanisms may not be reflected in this document. Changes may have been made to this work since it was submitted for publication. A definitive version was subsequently published in Lithos, Vol.190-191, (2014)].  
DOI: 10.1016/j.lithos.2013.11.015

1 **Partial melting of metabasic rocks in Val Strona di Omegna, Ivrea Zone,**  
2 **northern Italy**

3

4 Barbara E. Kunz <sup>a,1,\*</sup>, Tim E. Johnson <sup>a</sup>, Richard W. White <sup>a</sup>, Charlotte Redler <sup>b</sup>

5

6 <sup>a</sup> Earth System Science Research Centre, Institute for Geosciences, University of Mainz, Becherweg 21, D-  
7 55099, Mainz, Germany

8 <sup>b</sup> Institute of Earth and Environmental Sciences, University of Freiburg, Albertstrasse 23b, D-79104 Freiburg,  
9 Germany

10

11 \*Corresponding author. Tel.: +41 (0)31-631 4738; fax: +41 (0)31 631 4843.

12 E-mail address: barbara.kunz@geo.unibe.ch (B.E. Kunz).

13 <sup>1</sup> Present address: Institute of Geological Sciences, University of Bern, Baltzerstrasse 1+3, CH-3012 Bern,  
14 Switzerland.

15

16 **ABSTRACT**

17

18 Field and petrographic observations combined with major and trace element bulk rock  
19 geochemistry show that metabasic rocks within Val Strona di Omegna in the central Ivrea  
20 Zone partially melted during granulite facies regional metamorphism. A transition from  
21 granoblastic amphibolite facies metabasic rocks at the lowest metamorphic grades to  
22 metatexitic and diatexitic migmatites in the granulite facies records the effects of *in situ* fluid-  
23 absent partial melting. Coarse-grained euhedral clinopyroxene porphyroblasts within  
24 leucosomes are consistent with anatexis via incongruent fluid-absent melting reactions  
25 consuming hornblende, plagioclase and quartz to form clinopyroxene and melt. Field  
26 observations are supported by bulk rock geochemistry, in which high-grade samples are  
27 generally depleted in mobile elements relative to unmigmatized mid amphibolite facies rocks

28 that may approximate pre-melting protolith compositions. Many of the metabasic rocks at the  
29 highest-grade parts of Val Strona di Omegna probably belong to the Kinzigite Formation and  
30 are unlikely to be part of the younger Mafic Complex as previously proposed.

31

32 **Keywords:** *In situ* partial melting, metabasic rocks, granulite facies regional metamorphism,  
33 Ivrea Zone

34

35

## 36 **1. Introduction**

37

38 The main driving forces for differentiation of the Earth are partial melting and  
39 buoyancy-driven migration of melt. These processes are irreversible and have led to the  
40 pronounced physico-chemical structure of the continental crust (e.g., Brown and Rushmer,  
41 2006; Sawyer et al., 2011). As direct observation of these processes is not possible,  
42 information regarding pressure–temperature ( $P$ – $T$ ) conditions, melt compositions and the  
43 degree and mechanisms of the production, segregation and migration of melt are largely  
44 derived from the study of migmatites (e.g., Sawyer, 2008).

45 The Ivrea Zone in northern Italy (Fig. 1) exposes a section through the mid to lower  
46 continental crust and has been the focus of numerous studies, most of which have  
47 concentrated either on metapelitic rocks within the Kinzigite Formation (e.g., Barboza and  
48 Bergantz, 2000; Bertolani, 1968; Ewing et al., 2013; Handy et al., 1999; Luvizotto and Zack,  
49 2009; Mehnert, 1975; Redler et al., 2012, 2013; Zingg, 1978) or on the layered mafic  
50 intrusions from the Mafic Complex (e.g., Peressini et al., 2007; Quick et al., 1992, 1994,  
51 2009; Rivalenti et al., 1975, 1981; Sinigoi et al., 2011). The river section of Val Strona di  
52 Omegna preserves a near-continuous metamorphic field gradient from mid-amphibolite to  
53 granulite facies conditions in which metapelitic compositions preserve a transition from

54 unmelted (subsolidus) to partially melted (migmatitic) rocks (e.g., Redler et al., 2012, 2013;  
55 Schmid and Wood, 1976; Zingg, 1980). This study focusses on metabasic rocks that are  
56 interlayered with the metapelitic rocks in the Kinzigite Formation and which, though  
57 volumetrically abundant, have received relatively little attention (Reinsch, 1973a,b; Rushmer,  
58 1991; Sills and Tarney, 1984). Emphasis is on detailed field and petrographic observations  
59 augmented with whole rock geochemical data that together provide evidence that, along with  
60 the metapelitic rocks, the metabasic rocks within Val Strona di Omegna partially melted  
61 during high temperature regional metamorphism.

62

## 63 **2. Geological setting**

64

65         The Ivrea Zone is a NW dipping and NE–SW striking slice of pre-Alpine metamorphic  
66 basement located in northern Italy. It is bordered to the northwest by the Insubric Line (also  
67 known as the Periadriatic Line) that separates it from Alpine Units of the Canavese and Sesia  
68 Zones (Gansser, 1968), (Fig. 1). The Insubric Line is a 1–2 km wide zone of intense  
69 mylonitisation forming part of a major tectonic structure that can be traced from the French  
70 Alps in the west to Greece in the east, and which separates the Central/Western Alps from the  
71 Southern Alps (Gansser, 1968; Schmid et al., 1987). To the southeast, the Cossato-Mergozzo-  
72 Brissago Line (CMB Line) and the younger Pogallo Line separate the Ivrea Zone from the  
73 Strona-Ceneri Zone, which records greenschist to lower amphibolite facies assemblages and  
74 contains granitic plutons of Permian age and coeval volcanic rocks (Quick et al., 2009) that  
75 are locally covered by Mesozoic sediments. The Strona-Ceneri Zone represents a section  
76 through a shallower crustal level to that exposed in the Ivrea Zone (Boriani and Sacchi, 1973;  
77 Boriani et al., 1990), although it is unclear whether the Strona-Ceneri Zone and the Ivrea Zone  
78 represent a once contiguous crustal fragment or are discrete crustal terranes that were  
79 tectonically juxtaposed (Boriani and Sacchi, 1973).

80 In the southwestern part of the Ivrea Zone (Fig. 1), mafic rocks of the Mafic Complex  
81 and ultramafic rocks of the Balmuccia mantle peridotite crop out close to the Insubric Line  
82 (e.g., Quick et al., 1995, 2003; Rivalenti et al., 1975, 1981; Sinigoi et al., 1994, 2011). The  
83 Mafic Complex, which reaches a maximum thickness of around 8 km in Val Sesia, is a  
84 layered sequence of mafic/ultramafic rocks thought to have been formed by magmatic  
85 underplating in an extensional environment (Quick et al., 1992). The Mafic Complex has been  
86 subdivided into a lower unit, consisting mainly of amphibole gabbros and a ‘paragneiss-  
87 bearing belt’ in which the mafic rocks contain septa of paragneiss, and an upper unit, which is  
88 dominated by gabbros and diorites (Sinigoi et al., 1996).

89 The Kinzigite Formation crops out extensively within the central part of the Ivrea  
90 Zone and is best exposed in Val Strona di Omegna (Fig. 1). It is cross cut by the Mafic  
91 Complex in the southwest. The Kinzigite Formation comprises different rock types, the most  
92 common of which are metapelitic and metabasic rocks with subordinate metapsammite, calc-  
93 silicate, marble and metaperidotite. All rocks were regionally metamorphosed at amphibolite  
94 to granulite facies conditions (e.g., Barboza and Bergantz, 2000; Barboza et al., 1999; Henk et  
95 al., 1997; Peressini et al., 2007; Pin, 1990; Redler et al., 2012; Zingg, 1978) with regional  
96 assemblages overprinted by contact metamorphism in close proximity to gabbroic rocks of the  
97 Mafic Complex (e.g., Barboza and Bergantz, 2000; Barboza et al., 1999; Redler et al., 2012).

98 The pre-metamorphic history of the Kinzigite Formation is unclear, as the high-grade  
99 metamorphism and deformation have erased almost all evidence for older events (e.g.,  
100 Schmid, 1993; Vavra et al., 1999). Peressini et al. (2007) date the intrusion of the Mafic  
101 Complex to  $288 \pm 4$  Ma and high-grade metamorphism in the Kinzigite Formation to  $309 \pm 3$   
102 Ma. More recent work by Ewing et al. (2013) suggests regional granulite facies  
103 metamorphism in Val Strona di Omegna occurred at  $316 \pm 3$  Ma. *P–T* estimates from the  
104 Kinzigite Formation are mostly based on metapelitic samples and range from  $\sim 600^\circ\text{C}$  and 3–4  
105 kbar for the lowest grade rocks to in excess of  $900^\circ\text{C}$  and 10–12 kbar for the highest grade

106 granulite facies rocks (e.g., Bea and Montero, 1999; Ewing et al., 2013; Hunziker and Zingg,  
107 1980; Luvizotto and Zack, 2009; Redler et al., 2012; Schmid et al., 1987).

108 A detailed petrographic study in Val Strona di Omegna (Reinsch, 1973a) subdivided  
109 the metabasic rocks within the Kinzigite Formation (from relatively low to high grade) into:  
110 (i) amphibolites dominated by hornblende and plagioclase with minor quartz and biotite; (ii)  
111 garnetiferous metagabbros ('banded pyriboleites') containing plagioclase, garnet, hornblende  
112 and pyroxene and; iii) rare 'pyriclasites' containing plagioclase, clino- and orthopyroxene,  
113 quartz and biotite. Based on their bulk rock major element composition, Reinsch (1973b)  
114 classified the amphibolites as having alkali-basaltic to dacitic protoliths and the garnetiferous  
115 metagabbro and 'pyriclasites' as representing metamorphosed alkali to hypersthene-bearing  
116 basalts.  $P$ - $T$  conditions were estimated at 700°C and 4–6 kbar for the amphibolite facies  
117 metabasic rocks and 750–850°C and 6–8 kbar for the granulite facies metabasic rocks  
118 (Reinsch, 1973b). Using trace element geochemistry, Sills and Tarney (1984) identified two  
119 separate groups of amphibolites within Val Strona di Omegna. Type 1 amphibolites have trace  
120 element patterns similar to N-MORB while type 2 amphibolites show patterns similar to E-  
121 MORB.

122

### 123 **3. Field and petrographic observations**

124

125 The metabasic rocks in Val Strona di Omegna commonly occur as elongate lenses  
126 ranging in width from 10 cm to around 100 m that are interlayered with the metapelitic rocks.  
127 Based on changes in mineral assemblages, the valley can be subdivided into three different  
128 sections based on metamorphic (sub)facies: the mid amphibolite facies, the upper amphibolite  
129 facies and the granulite facies (Fig. 2). The major mineral assemblage of samples is given in  
130 Table 1. Mineral abbreviations follow Kretz (1983) and migmatite terminology follows  
131 Sawyer (2008).

132

133 *3.1. Mid amphibolite facies*

134

135 Mid amphibolite facies rocks are exposed from the lowest grade outcrops close to the  
136 CMB Line at the village of Germagno to the village of Marmo, some six kilometres to the  
137 northwest (Fig. 2). The upper (higher grade) boundary of the mid amphibolite facies is  
138 defined by the first obvious occurrence of clinopyroxene in metabasic rocks, which occurs  
139 close to the K-feldspar in/muscovite out isograd in metapelitic rocks (Redler et al., 2012).  
140 Within this section, the metabasic rocks occur as weakly-foliated NE–SW oriented pods and  
141 lenses in which secondary veins of quartz or calcite are common (Fig. 3a). Some samples  
142 contain porphyroblasts of hornblende or, rarely, garnet, and some preserve a foliation defined  
143 by biotite and hornblende (Fig. 4a). No macroscopic or microscopic evidence for partial  
144 melting has been identified in metabasic rocks in the mid amphibolite facies.

145 The typical mineral assemblage of mid amphibolite facies metabasic rocks is (green)  
146 hornblende, plagioclase, quartz, biotite and ilmenite (Table 1), with garnet additionally  
147 present in one sample (IZ 027). K-feldspar, chlorite, pyrite, apatite, chalcopyrite, hematite,  
148 zircon and/or calcite occur as minor or accessory phases. Hornblende (typically 0.1–10 mm in  
149 length) is lepidoblastic and pleochroic from intense green to beige and may be partially to  
150 completely replaced by biotite (Fig. 4a). Plagioclase (0.1–2 mm) is anhedral and is commonly  
151 partially seriticised. Quartz (< 0.1–5 mm) is granoblastic and exhibits undulose extinction.  
152 Biotite (0.1–3.5 mm) is pleochroic from dark brown to beige and has a lepidoblastic habit  
153 (Fig. 4a). Ilmenite and other opaque phases have a maximum length of 0.5 mm, are  
154 commonly elongated subparallel to the foliation and occur both within the matrix and as  
155 inclusions in hornblende and garnet. Garnet within sample IZ 027 (0.5–3.5 mm) is skeletal  
156 and contains numerous inclusions of ilmenite and hornblende.

157

158 3.2. *Upper amphibolite facies*

159

160 The upper amphibolite facies section is here defined as the section of the valley  
161 between the first noted occurrence of clinopyroxene (north of the village of Marmo) to the  
162 first appearance of orthopyroxene (near the village of Forno) in metabasic rocks (Fig. 2), and  
163 is elsewhere referred to as the 'Transition Zone' (Bea and Monero, 1999). At the lower-grade  
164 end there is no obvious macroscopic change in the appearance of the metabasic rocks relative  
165 to lower-grade rocks. Approximately one kilometre northwest of the village of Marmo (Fig.  
166 2), the metabasic rocks contain segregations concentrating either leucocratic or melanocratic  
167 minerals that occur as layers aligned subparallel to the foliation. Towards higher grades, south  
168 of the village of Rosarolo (Fig. 2), the metabasic rocks become more granoblastic and the first  
169 clear evidence for *in situ* partial melting is visible. Small quartzofeldspathic leucocratic  
170 patches (leucosome) with a diameter of 2–5 cm occur with and/or enclose pale green  
171 clinopyroxene porphyroblasts (5–35 mm in diameter) (Fig. 3b). Melanocratic layers  
172 (melanosome) are dominated by green-brown hornblende with minor plagioclase and quartz.  
173 At the high-grade end of the upper amphibolite facies section, south of Forno (Fig. 2), discrete  
174 clinopyroxene-bearing leucosome veins cross-cut the foliation (Fig. 3c).

175 The main mineral assemblage of the upper amphibolite facies metabasic rocks is  
176 clinopyroxene, green/brown hornblende, plagioclase, quartz and ilmenite (Table 1). Minor  
177 and accessory phases include sphene, garnet, rutile, biotite, zircon, chlorite, pyrite, calcite,  
178 chalcopyrite, hematite and/or apatite. In thin section, subhedral, near-colourless clinopyroxene  
179 ranges in size from 0.5 mm in the matrix to porphyroblasts up to 35 mm across (Fig. 4b). In  
180 some samples clinopyroxene is extensively replaced by hornblende. Strongly-pleochroic  
181 anhedral to euhedral hornblende (0.5–5.5 mm) occurs as both green and brown variants, in  
182 which the proportion of brown hornblende increases upgrade. Close to the granulite facies  
183 transition only brown hornblende is present. Plagioclase (0.5–4.5 mm) and quartz (average 0.5



184 mm but up to 10 mm) are anhedral. Ilmenite and other opaque phases occur as sub-rounded  
185 grains up to 1 mm across.

186

### 187 *3.3. Granulite facies*

188

189 Granulite facies assemblages are preserved in rocks from the village of Forno to the  
190 Insubric Line northwest of Campello Monti (Fig. 2). Granulite facies metabasic rocks have a  
191 coarser grain size compared with amphibolite facies rocks and contain conspicuous  
192 porphyroblasts of clinopyroxene up to 5 cm and garnet up to 10 cm in diameter (Fig. 3d–j).  
193 Field relationships between the different rock types are complex due to an inferred increase in  
194 the degree of partial melting of both metapelitic and metabasic rocks. Close to lithological  
195 contacts metabasic rocks commonly contain veins and patches of leucosome derived from the  
196 metapelitic rocks, and the origin of individual leucosomes may be ambiguous (Redler et al.,  
197 2013).

198 Most leucosomes occur as veins (millimetres to decimetres thick) that form either  
199 interconnected networks or more irregular bodies concentrated within interboudin partitions  
200 or folds hinges (Fig. 3d–i). Leucosomes generated within, or derived from, the metabasic  
201 rocks are mostly dominated by plagioclase and quartz and contain peritectic clinopyroxene  
202 that is partly retrogressed to hornblende (Fig. 3h, j). The melanosome is generally dominated  
203 by clinopyroxene and garnet with varying amounts of orthopyroxene, hornblende and biotite.  
204 In some places hornblende-rich selvages are spatially associated with leucosome and form  
205 irregular patches a few centimetres across (Fig. 3h). Some of the rocks preserve scarce field  
206 evidence for partial melting (i.e. they lack obvious leucosome), although in thin section these  
207 samples have residual mineral assemblages dominated by pyroxene and garnet with little to  
208 no amphibole and plagioclase. However, most granulite facies metabasic rocks are

209 metatexites, comprising stromatic or patch migmatites. Metabasic diatexites are rare and  
210 occur locally only at the highest grades.

211         Granulite facies metabasic rocks contain clinopyroxene, orthopyroxene, brown  
212 hornblende, plagioclase, biotite, ilmenite, garnet and quartz (Table 1), with minor rutile,  
213 sphene, zircon, K-feldspar, hematite, chlorite, pyrite, chalcopyrite, apatite and/or calcite.  
214 Matrix clinopyroxene occurs most commonly as subhedral grains with an average size of 0.5  
215 mm (Fig. 4c–f). Clinopyroxene porphyroblasts are euhedral, up to 35 mm across, and may  
216 contain exsolution lamellae of orthopyroxene. In the highest-grade sample (IZ 100),  
217 clinopyroxene is pale green in thin section. Clinopyroxene may contain inclusions of garnet,  
218 ilmenite and biotite and is commonly partially to completely replaced by hornblende, which is  
219 itself commonly replaced by biotite (Fig. 4h). Orthopyroxene (<0.5–2 mm in the matrix) is  
220 morphologically similar to clinopyroxene, although in most samples orthopyroxene is much  
221 less abundant (Fig. 4 c–f). Porphyroblasts of orthopyroxene with a grain size larger than 5 mm  
222 are uncommon. Hornblende forms granoblastic subhedral to euhedral grains that are  
223 pleochroic from dark brown to beige and range in size from < 0.25 mm in the matrix to  
224 porphyroblasts up to 5 mm across (Fig. 4c–h).

225         Where present, garnet mostly occurs as subhedral, skeletal porphyroblasts up to 5 mm  
226 across containing numerous inclusions of hornblende, clinopyroxene, orthopyroxene,  
227 plagioclase, biotite, quartz and ilmenite (Fig. 4 c,d,g). In the highest-grade samples, garnet  
228 occurs as euhedral pale pink crystals with a grain size of 5–100 mm. These large garnet  
229 porphyroblasts are commonly surrounded by a layered corona with an inner plagioclase-rich  
230 layer and outer hornblende-rich layer (Fig. 4g). Lepidoblastic biotite (0.1–1 mm) is more  
231 common in the granulite facies metabasic rocks relative to upper amphibolite facies samples.  
232 Plagioclase within the melanosome is anhedral to subhedral with an average grain size of 1  
233 mm; quartz is mostly subhedral, shows undulose extinction and has a maximum grain size of  
234 0.1 mm. In leucosome veins, plagioclase and quartz can be several centimetres across.

235 Ilmenite is coarse grained (up to 1 mm) and commonly occurs as inclusions in garnet,  
236 pyroxene or hornblende.

237

#### 238 **4. Whole rock geochemistry**

239

##### 240 *4.1. Analytical Methods*

241

242 Bulk rock major and trace element compositions of 31 samples were determined by X-  
243 ray fluorescence spectroscopy (XRF) and Laser Ablation Inductively Coupled Plasma Mass  
244 Spectrometry (LA-ICP-MS) at the Institute for Geoscience, University of Mainz. For XRF  
245 analysis, a representative unaltered part of the sample was crushed and milled to a grain size  
246 of less than 63  $\mu\text{m}$ . 0.4 g of the sample powder was mixed with 5.2 g of flux ( $\text{Li}_2\text{B}_4\text{O}_7$ )  
247 (corresponding to a 14-times dilution) and fused to glass beads in a Pt-cylinder. Samples were  
248 analysed by X-ray fluorescence using a Philips Magix Pro for  $\text{SiO}_2$ ,  $\text{Al}_2\text{O}_3$ , Fe(total), MnO,  
249 MgO, CaO,  $\text{Na}_2\text{O}$ ,  $\text{K}_2\text{O}$ ,  $\text{TiO}_2$ ,  $\text{P}_2\text{O}_5$ ,  $\text{SO}_3$ ,  $\text{Cr}_2\text{O}_3$  and NiO. Accuracy for major element  
250 concentrations was <1 % relative except for MnO (2 %) and  $\text{Na}_2\text{O}$  (1.5 %). The loss on  
251 ignition (LOI) was taken as a direct proxy for the  $\text{H}_2\text{O}$  content. Selected trace element (Sc, Cr,  
252 Ni, Rb, Pb) were also measured by XRF, in which 6 g of the rock powder were mixed with  
253 two component epoxy and pressed to a tablet. The trace elements Cs, Ba, Th, U, Nb, Ta, La,  
254 Ce, Pr, Nd, Sr, Sm, Hf, Zr, Ti, Eu, Gd, Dy, Ho, Y, Er, Yb and Lu were determined by LA-  
255 ICP-MS. Sample powders were fused to glass beads on an iridium strip heater under an Ar-  
256 atmosphere (Nehring et al., 2008) then analysed with an Agilent 7500 quadrupole ICP-MS  
257 coupled with a New Wave Research UP-193nm laser ablation system. The background was  
258 measured for 30 s prior to sample analysis. Standardisation after every 10th measured spot  
259 used standard NIST SRM 612. Ca values measured by XRF were used as an internal standard.  
260 At the beginning and the end of the analytical run, standard NIST SRM 610 was measured to

261 ensure consistency. Data reduction used the software 'Glitter'. Table 2 gives the major and  
262 trace element composition for eight representative samples from Val Strona di Omegna.

263

#### 264 *4.2. Major elements*

265

266 Figure 5 shows selected major element oxide variation diagrams for the metabasic  
267 rocks. Although there is considerable variation in the composition of samples, some general  
268 trends are recognisable. SiO<sub>2</sub> contents range between 41 and 56 wt%, in which the mid  
269 amphibolite facies samples generally have the highest SiO<sub>2</sub> contents, with rocks from higher  
270 grades relatively depleted in SiO<sub>2</sub>. A similar trend is observed for K<sub>2</sub>O contents (0.3–1.5  
271 wt%), which are highest in the mid amphibolite facies rocks and lowest in the granulite facies  
272 rocks. Although there is significant overlap, the concentrations of TiO<sub>2</sub> (0.6–3.2 wt%), Al<sub>2</sub>O<sub>3</sub>  
273 (13–24 wt%), CaO (6–17 wt%), total iron as FeO (6–19 wt%) and MgO (2.0–8.5 wt%)  
274 generally increase from low- to high-grade samples. Concentrations of MnO (0.07–0.4 wt%)  
275 and Na<sub>2</sub>O (0.5–3.7 wt%) are highly variable and exhibit no clear correlation with  
276 metamorphic grade.

277

#### 278 *4.3. Trace elements*

279

280 There is considerable variability in the trace element composition of samples. Figure 6  
281 shows concentrations of selected trace elements within the metabasic rocks normalised to  
282 primitive mantle (PM) values (McDonough and Sun, 1995) with elements ordered by  
283 increasing compatibility in oceanic basalts (Hofmann, 1988). The composition of average N-  
284 MORB, E-MORB (Hofmann, 1988; Sun and McDonough, 1989) and of the middle and lower  
285 continental crust (Rudnick and Gao, 2003) are shown for reference.

286 Samples from the mid amphibolite facies (Fig. 6a) have trace element concentrations  
287 that generally fall within the compositional range of average middle to lower continental  
288 crust, although two samples are relatively enriched in Nb and Ta. The Hf and Zr  
289 concentrations show two distinct groups, one with concentrations similar to average middle  
290 continental crust and another with trace element compositions depleted with respect to N-  
291 MORB. Samples from the upper amphibolite facies samples (Fig. 6b) generally show less  
292 variability than mid amphibolite and granulite facies samples. With the exception of Ba, Th  
293 and Sr, LILE are enriched in upper amphibolite rocks compared to N-MORB whereas other  
294 trace elements have concentrations between average N- and E-MORB. The granulite facies  
295 samples show the most variable trace element compositions (Fig. 6c). With the exception of  
296 four samples that show a strong negative Th anomaly, all are enriched in LILE compared to  
297 N-MORB. Similar to mid amphibolite facies samples, granulite facies samples can be  
298 separated into two groups based on their Nb, Ta and Hf, Zr contents.

299 Figure 7 shows rare earth element (REE) concentrations in metabasic rocks from Val  
300 Strona di Omegna normalised to CI chondrite values (Sun and McDonough, 1989).  $(La/Lu)_N$   
301 ratios are variable in both mid amphibolite facies (1.1–10.5) and granulite facies (1.0–8.8)  
302 samples. However, upper amphibolite facies samples generally have more uniform REE  
303 patterns with  $(La/Lu)_N < 1$ ,  $(La/Sm)_N < 1$  and  $(Gd/Lu)_N \sim 1$ . With the exception of one sample,  
304 upper amphibolite facies samples show REE patterns similar to average N-MORB. The LREE  
305 concentrations in the mid amphibolite facies show two distinct trends; three samples show  
306 concentrations similar to average E-MORB and lower continental crust with  $(La/Sm)_N$  ratios  
307 of 0.7–1.4 whereas three others have values comparable to average middle continental crust,  
308 with  $(La/Sm)_N$  ratios of 2.6–3.6. The HREE patterns in the mid amphibolite facies are flat  
309 with  $(Gd/Lu)_N$  ratios between 1.1–2.6, similar to granulite facies samples [ $(Gd/Lu)_N = 1–3$ ].  
310 Most granulite facies samples show relative flat LREE patterns with  $(La/Sm)_N$  ratios of 0.5–  
311 2.4 but range from compositions similar to N-MORB to samples with concentrations higher

312 than those in average middle continental crust. Pronounced europium anomalies are not  
313 evident in the metabasic rocks from Val Strona di Omegna ( $\text{Eu}/\text{Eu}^*=0.5\text{--}1.5$ ). Two mid  
314 amphibolite facies samples and two-thirds of granulite facies samples show a small negative  
315 europium anomaly whereas no europium anomaly is evident in upper amphibolite facies  
316 samples. A comparison of the bulk rock trace element composition (Fig. 6d; 7d) of metabasic  
317 rocks sampled close to Campello Monti (this study; Fig. 2) and mafic rocks from the Mafic  
318 Complex (taken from Sinigoi et al., 2011) show large variability in which a clear  
319 compositional distinction between rocks within the Kinzigite Formation and the Mafic  
320 complex cannot be made.

321

## 322 **6. Discussion**

323

324 Studies of migmatites provide physico-chemical constraints on the processes of melt  
325 production, segregation and migration. Peak temperatures in excess of  $700^\circ\text{C}$  are commonly  
326 recorded by rocks in the highest-grade parts of regional metamorphic belts, in which  
327 numerous studies have documented evidence for fluid-absent partial melting of metapelitic  
328 rocks (e.g., Sawyer, 2008). However, under ‘normal’ (Barrovian) regional metamorphic  
329 geothermal gradients, and in the absence of an external supply of  $\text{H}_2\text{O}$ -rich fluids, much  
330 higher temperatures ( $>$  or  $\gg 800^\circ\text{C}$ ; Rushmer, 1991; Wyllie and Wolf, 1993) are required to  
331 produce significant quantities of melt from metabasic rocks. Petrological studies pertaining to  
332 the partial melting of these common mafic crustal protoliths are scarce (e.g., Hartel and  
333 Pattison, 1996; Johnson et al., 2012; Sawyer, 1991).

334 The results presented in this study show a broadly consistent mineralogical, textural  
335 and geochemical evolution from mid amphibolite to granulite facies conditions that support  
336 the interpretation that metabasic rocks within Val Strona di Omegna partially melted during  
337 high temperature regional metamorphism. Temperature estimates using the Zr-in-rutile

338 thermometer (Ewing et al., 2013; Luvizotto and Zack, 2009) and phase equilibria modelling  
339 of metapelitic rocks (Redler et al., 2012) indicate maximum metamorphic peak temperature  
340 conditions in excess of 900°C in Val Strona di Omegna. Such temperatures are sufficiently  
341 high that fluid-absent melting of metabasic lithologies via the incongruent breakdown of  
342 hornblende is inevitable at the highest metamorphic grades, providing the protoliths were  
343 sufficiently hydrated (Rushmer, 1991; Wyllie and Wolf, 1993).

344         Field observations provide unequivocal evidence that most of the high grade metabasic  
345 rocks within the Kinzigite Formation underwent *in situ* partial melting (Fig. 3). Mineral  
346 assemblages in the mid amphibolite facies are dominated by green-hornblende and  
347 plagioclase and the rocks preserve no clear evidence for partial melting. In the upper  
348 amphibolite facies the metabasic rocks additionally contain clinopyroxene and patches of  
349 quartzofeldspathic leucosome segregations containing centimetric clinopyroxene  
350 porphyroblasts that are significantly larger than clinopyroxene within the melanosome and  
351 which are interpreted as the solid (peritectic) product of the fluid-absent breakdown of  
352 hornblende, plagioclase and quartz to form clinopyroxene and melt (Fig. 3j–l; 4b; Johnson et  
353 al., 2012). These porphyroblast–leucosome relationships are consistent with the *in-situ*  
354 spatially-focussed formation of melt around the porphyroblasts (e.g., White et al., 2004;  
355 White, 2008). Close to the granulite facies boundary the metabasic rocks contain fine-grained  
356 stromatic leucosomes as well as coarse-grained, peritectic clinopyroxene-bearing leucosomes  
357 that cross cut the foliation (Fig. 3c). Granulite facies metabasic rocks contain near anhydrous  
358 assemblages dominated by clinopyroxene, garnet and plagioclase, with or without  
359 orthopyroxene, and exhibit features suggesting highly variable degrees of partial melting that  
360 are likely related to either the original H<sub>2</sub>O content of the protoliths (i.e. the amount of  
361 amphibole ± biotite stable on crossing the solidus) and/or the textural development during  
362 melting and the efficacy of melt loss. Leucosome contents in granulite facies metabasic rocks  
363 are 10–20 vol.% that, if produced *in situ* or in source, provide a minimum estimate on melt

364 productivity. The limited degree of retrograde replacement of anhydrous minerals in rocks  
365 preserving evidence for partial melting requires loss of melt (White and Powell, 2002).

366         Although the major and trace element data show a large degree of scatter and overlap,  
367 the data are consistent with an interpretation of partial melting and melt loss. Figure 8 shows  
368 average major and trace element data of the upper amphibolite and granulite facies samples  
369 normalised to the average mid amphibolite facies samples. Assuming the average composition  
370 of mid amphibolite facies samples is a reasonable approximation for that of the unmelted  
371 protoliths, Fig. 8 shows an overall relative depletion in Na, K, LILE and possibly Si, Al and  
372 LREE in upper amphibolite and granulite facies rocks, mobile elements which are  
373 incompatible and will partition preferentially into the melt. In contrast, the more compatible  
374 elements Mg, Ca, Fe, Ti, HFSE and HREE are relatively enriched in the high-grade samples  
375 relative to their inferred protolith, consistent with these compositions representing residua  
376 following partial melting and melt loss.

377         However, upper amphibolite facies samples are in general more depleted in fluid  
378 mobile elements and more enriched in residual elements relative to the granulite facies  
379 samples (Fig. 8), which is inconsistent with a simple interpretation of partial melting and melt  
380 loss from compositions similar to an average lower amphibolite facies protolith. In addition,  
381 most granulite facies samples contain minor biotite whereas upper amphibolite facies samples  
382 do not. These differences might suggest different protolith compositions for upper  
383 amphibolite facies rocks relative to mid amphibolite and granulite facies rocks (e.g., Sills &  
384 Tarney, 1984). Another plausible explanation could be the variable abundance of metapelitic  
385 rocks within Val Strona di Omegna. The detailed geological map of Bertolani (1968) shows  
386 that the proportion of metapelitic to metabasic rocks is high in the mid amphibolite and  
387 granulite facies sections relative to those in the upper amphibolite facies, where metabasic  
388 rocks dominate. At the highest metamorphic grades, where residual (i.e. melt-depleted)  
389 metapelitic rocks are volumetrically dominant (Schmid and Wood, 1976), nearby metabasic



390 rocks are more likely to have interacted with metapelite-derived melt, leading to a relative  
391 enrichment in mobile elements and the growth of biotite. In upper amphibolite facies rocks,  
392 where metapelitic rocks are far less abundant, contamination with metapelite-derived  
393 components was more restricted, perhaps explaining why the rocks did not develop biotite.

394         Metabasic rocks throughout the Ivrea Zone have a range of compositions that likely  
395 reflect complex magmatic process (e.g., heterogeneity of the source and fractionation) as well  
396 as variable degrees of interaction with and contamination by crustal material during prograde  
397 metamorphism (in case of pre- to syn metamorphic metabasic rocks) or emplacement (in the  
398 case of the mafic rocks within the Mafic Complex, Correia et al., 2012, Sinigoi et al., 2011).  
399 More detailed investigations (including isotopic analysis) are required to better constrain their  
400 petrogenesis. However, many metabasic rocks within Val Strona di Omegna have mineral  
401 assemblages consistent with metamorphic conditions constrained from the metapelitic rocks  
402 (e.g., Redler et al., 2012). In addition, prograde metamorphic features in these metabasic rocks  
403 are consistent with their protoliths having been emplaced and hydrated prior to, or at least in  
404 the early stages of, prograde metamorphism. The evidence for *in situ* melting and the  
405 occurrence of hornblende inclusions in porphyroblasts is consistent with these rocks having  
406 been sufficiently hydrous that they contained a substantial quantity amphibole during  
407 prograde metamorphism. Thus, many of the metabasic rocks in Val Strona di Omegna section  
408 experienced an identical prograde, peak and retrograde metamorphic history as the  
409 metasedimentary rocks that host them.

410         Previous studies have attributed all metabasic rocks around Campello Monti to the  
411 Mafic Complex (e.g., Capedri et al., 1977) whereas other ascribe all metabasic rocks in Val  
412 Strona di Omegna to the Kinzigite Formation (e.g., Bertolani, 1968). This study suggests that  
413 some of the metabasic rocks around Campello Monti show no distinct difference in  
414 metamorphic evolution, mineral assemblages, migmatite textures or whole rock composition

415 when compared with other granulite facies rocks within the Kinzigite Formation, and these  
416 rocks should probably not be regarded as part of the Mafic Complex.

417

## 418 **7. Conclusions**

419

- 420 • Metabasic rocks within the Kinzigite Formation in Val Strona di Omegna show a  
421 continuous evolution from mid amphibolite facies to granulite facies conditions, the  
422 result of high-grade regional metamorphism;
- 423 • At the highest grades the metabasic rocks are migmatites, in which a close spatial  
424 relationship between leucosome and coarse-grained euhedral clinopyroxene provides  
425 evidence for *in situ* partial melting by reactions consuming hornblende, plagioclase  
426 and quartz;
- 427 • The bulk rock geochemistry of metabasic rocks within the Kinzigite Formation  
428 support an interpretation of partial melting and melt loss with variable interaction with  
429 melt derived from surrounding metapelitic rocks;
- 430 • Many of the metabasic rocks within the Kinzigite Formation were emplaced and  
431 hydrated prior to or during prograde metamorphism permitting *in situ* partial melting.  
432 They followed a similar metamorphic history (prograde, peak and retrograde) to the  
433 metasedimentary rocks in Val Strona di Omegna;
- 434 • Many of the metabasic rocks at the highest metamorphic grades within Val Strona di  
435 Omegna should be regarded as part of the Kinzigite Formation, not the Mafic  
436 Complex as previously proposed (e.g., Capedri et al., 1977).

437

## 438 **Acknowledgements**

439

440 We thank D. Jacob and N. Groschopf for their help with whole rock and mineral  
441 geochemical analyses. We are grateful to S. Sinigoi and an anonymous reviewer for their  
442 helpful and perceptive reviews and to M. Scambelluri for his editorial handling.

443

#### 444 **References**

445 Barboza, S.A., Bergantz, G.W., 2000. Metamorphism and anatexis in the Mafic Complex  
446 contact aureole, Ivrea Zone, Northern Italy. *Journal of Petrology* 41, 1307-1327.

447 Barboza, S.A., Bergantz, G.W., Brown, M., 1999. Regional granulite facies metamorphism in  
448 the Ivrea zone: Is the Mafic Complex the smoking gun or a red herring?. *Geology* 27, 447-  
449 450.

450 Bea, F., Montero, P., 1999. Behavior of accessory phases and redistribution of Zr, REE, Y,  
451 Th, and U during metamorphism and partial melting of metapelites in the lower crust: an  
452 example from the Kinzigite Formation of Ivrea-Verbano, NW Italy. *Geochimica et*  
453 *Cosmochimica Acta* 63, 1133-1153.

454 Bertolani, M., 1968. La petrografia della Valle Strona (Alpi Occidentali Italiane).

455 *Schweizerische Mineralogische und Petrographische Mitteilungen* 48, 695-733.

456 Bigi, G., Castellarin, A., Coli, M., Dal Piaz, G.V., Sartori, R., Scandone, P., 1990. Structural  
457 model of Italy sheet 1, 1:500000. Consiglio Nazionale delle Ricerche, Progetto Finalizzato  
458 Geodinamica, SELCA Firenze.

459 Boriani, A., Giobbi Origoni, E., Borghi, A., Caironi, V., 1990. The evolution of the "Serie dei  
460 Laghi" (Strona-Ceneri and Scisti dei Laghi): the upper component of the Ivrea-Verbano  
461 crustal section; Southern Alps, North Italy and Ticino, Switzerland. *Tectonophysics* 182,  
462 103-118.

463 Boriani, A., Sacchi, R., 1973. Geology of the junction between the Ivrea-Verbano and Strona-  
464 Ceneri Zones. *Memorie degli Istituti di Geologia e Mineralogia dell'Universita di Padova*  
465 28, 1-36.

466 Brown, M., Rushmer, T., 2006. Evolution and differentiation of the continental crust.  
467 Cambridge University Press.

468 Capedri, S., Coradini, A., Fanucci, O., Garuti, G., Rivalenti, G., Rossi, A., 1977. The origin of  
469 the Ivrea-Verbanò Basic Formation (Italian Western Alps). Statistical approach to the  
470 peridotite problem. *Rendiconti della Società Italiana di Mineralogia e Petrologia* 33, 583-  
471 592.

472 Correia, C.T., Sinigoi, S., Girardi, V.A.V., Mazzucchelli, M., Tassinari, C.C.G., Giovanardi,  
473 T., 2012. The growth of large mafic intrusions: Comparing Niquelândia and Ivrea igneous  
474 complexes. *Lithos* 155, 167-182.

475 Ewing, T.A., Hermann, J., Rubatto, D., 2013. The robustness of the Zr-in-rutile and Ti-in-  
476 zircon thermometers during high-temperature metamorphism (Ivrea-Verbanò Zone,  
477 northern Italy). *Contributions to Mineralogy and Petrology* 4, 757-779.

478 Gansser, A., 1968. The Insubric line, a major geotectonic problem. *Schweizerische*  
479 *Mineralogische und Petrographische Mitteilungen* 48, 123-143.

480 Handy, M.R., Franz, L., Heller, F., Janott, B., Zurbriggen, R., 1999. Multistage accretion and  
481 exhumation of the continental crust (Ivrea crustal section, Italy and Switzerland).  
482 *Tectonics* 18, 1154-1177.

483 Hartel, T.H.D., Pattison, D.R.M., 1996. Genesis of the Kapuskasing (Ontario) migmatitic  
484 mafic granulites by dehydration melting of amphibolite: the importance of quartz to  
485 reaction progress. *Journal of Metamorphic Geology* 14, 591-611.

486 Henk, A., Franz, L., Teufel, S., Oncken, O., 1997. Magmatic Underplating, Extension, and  
487 Crustal Reequilibration: Insights from a Cross-Section through the Ivrea Zone and Strona-  
488 Ceneri Zone, Northern Italy. *The Journal of Geology* 105, 367-377.

489 Hofmann, A.W., 1988. Chemical differentiation of the Earth: the relationship between mantle,  
490 continental crust, and oceanic crust. *Earth and Planetary Science Letters* 90, 297-314.

491 Hunziker, J.C., Zingg, A., 1980. Lower Palaeozoic Amphibolite to Granulite Facies  
492 Metamorphism in the Ivrea Zone (Southern Alps, Northern Italy). Schweizerische  
493 Mineralogische und Petrographische Mitteilungen 60, 181-213.

494 Johnson, T.E., Fischer, S., White, R.W., Brown, M., Rollinson, H.R., 2012. Archaean  
495 Intracrustal Differentiation from Partial Melting of Metagabbro - Field and Geochemical  
496 Evidence from the Central Region of the Lewisian Complex, NW Scotland. Journal of  
497 Petrology 53, 2115-2138.

498 Kretz, R., 1983. Symbols for rock-forming minerals. American Mineralogist 68, 277-279.

499 Luvizotto, G.L., Zack, T., 2009. Nb and Zr behavior in rutile during high-grade  
500 metamorphism and retrogression: An example from the Ivrea-Verbano Zone. Chemical  
501 Geology 261, 303-317.

502 McDonough, W.F., Sun, S.s., 1995. The composition of the Earth. Chemical Geology 120,  
503 223-253.

504 Mehnert, K.R., 1975. The Ivrea Zone: A model of the deep crust. Neues Jahrbuch  
505 Mineralogische Abhandlungen 125, 156-199.

506 Nehring, F., Jacob, D.E., Barth, M.G., Foley, S.F., 2008. Laser-ablation ICP-MS analysis of  
507 siliceous rock glasses fused on an iridium strip heater using MgO dilution. Microchimica  
508 Acta 160, 153-163.

509 Peressini, G., Quick, J.E., Sinigoi, S., Hofmann, A.W., Fanning, M., 2007. Duration of a  
510 Large Mafic Intrusion and Heat Transfer in the Lower Crust: a SHRIMP U-Pb Zircon  
511 Study in the Ivrea-Verbano Zone (Western Alps, Italy). Journal of Petrology 48, 1185-  
512 1218.

513 Pin, C., 1990. Evolution of the lower crust in the Ivrea Zone: a model based on isotopic and  
514 geochemical data, in: Vielzeuf, D., Vidal, P. (Eds.). Kluwer Academic Publisher, pp. 87-  
515 110.

516 Quick, J.E., Sinigoi, S., Negrini, L., Demarchi, G., Mayer, A., 1992. Synmagmatic  
517 deformation in the underplated igneous complex of the Ivrea-Verbano zone. *Geology* 20,  
518 613-616.

519 Quick, J.E., Sinigoi, S., Mayer, A., 1994. Emplacement dynamics of a large mafic intrusion in  
520 the lower crust, Ivrea-Verbano Zone, northern Italy. *Journal of Geophysical Research* 99,  
521 21559-21573.

522 Quick, J.E., Sinigoi, S., Mayer, A., 1995. Emplacement of mantle peridotite in the lower  
523 continental crust, Ivrea-Verbano zone, northwest Italy. *Geology* 23, 739-742.

524 Quick, J.E., Sinigoi, S., Snoke, A.W., Kalakay, T.J., Mayer, A., Peressini, G., 2003. Geologic  
525 map of the southern Ivrea-Verbano Zone northwestern Italy. U.S. Geological Survey,  
526 Geologic Investigations Series Map I-2776, scale 1:25,000.

527 Quick, J.E., Sinigoi, S., Peressini, G., Demarchi, G., Wooden, J.L., Sbisà, A., 2009. Magmatic  
528 plumbing of a large Permian caldera exposed to a depth of 25 km. *Geology* 37, 603-606.

529 Redler, C., Johnson, T.E., White, R.W., Kunz, B.E., 2012. Phase equilibrium constraints on a  
530 deep crustal metamorphic field gradient: metapelitic rocks from the Ivrea Zone (NW  
531 Italy). *Journal of Metamorphic Geology* 30, 235-254.

532 Redler, C., White, R.W., Johnson, T.E., 2013. Migmatites in the Ivrea Zone (NW Italy):  
533 Constraints on partial melting and melt loss in metasedimentary rocks from Val Strona di  
534 Omega. *Lithos* 175-176, 40-53.

535 Reinsch, D., 1973a. Die Metabasite des Valle Strona (Ivrea Zone). *Neues Jahrbuch*  
536 *Mineralogische Abhandlungen* 118, 190-210.

537 Reinsch, D., 1973b. Die Metabasite des Valle Strona (Ivrea Zone) (2. Teil). *Neues Jahrbuch*  
538 *Mineralogische Abhandlungen* 119, 266-284.

539 Rivalenti, G., Garuti, G., Rossi, A., 1975. The origin of the Ivrea-Verbano Basic Formation  
540 (western Italian Alps) - whole rock geochemistry. *Bollettino della Società Geologica*  
541 *Italiana* 94, 1149-1186.

542 Rivalenti, G., Garuti, G., Rossi, A., Siena, F., Sinigoi, S., 1981. Existence of Different  
543 Peridotite Types and of a Layered Igneous Complex in the Ivrea Zone of the Western  
544 Alps. *Journal of Petrology* 22, 127-153.

545 Rudnick, R.L., Gao, S., 2003. Composition of the Continental Crust, in: Holland, H.D.,  
546 Turekian, K.K. (Eds.), *Treatise on Geochemistry*. Elsevier, pp. 1-64.

547 Rushmer, T., 1991. Partial melting of two amphibolites: contrasting experimental results  
548 under fluid-absent conditions. *Contributions to Mineralogy and Petrology* 107, 41-59.

549 Rutter, E., Brodie, K., James, T., Burlini, L., 2007. Large-scale folding in the upper part of the  
550 Ivrea-Verbano zone, NW Italy. *Journal of Structural Geology* 29, 1-17.

551 Sawyer, E.W., 1991. Disequilibrium Melting and the Rate of Melt - Residuum Separation  
552 During Migmatization of Mafic Rocks from the Grenville Front, Quebec. *Journal of*  
553 *Petrology* 32, 701-738.

554 Sawyer, E.W., 2008. *Atlas of Migmatites*. The Canadian Mineralogist, Special Publication,  
555 9. NRC Research Press, Ottawa, Ontario, Canada.

556 Sawyer, E.W., Cesare, B., Brown, M., 2011. When the continental crust melts. *Elements* 7,  
557 229-234.

558 Schmid, R., 1967. Zur Petrographie und Struktur der Zone Ivrea-Verbano zwischen Valle  
559 d'Ossola und Val Grande (Prov. Novara, Italien). *Schweizerische Mineralogische und*  
560 *Petrographische Mitteilungen* 47, 935-1117.

561 Schmid, S.M., 1993. Pre-Mesozoic geology in the Alps, in: von Raumer, J.F., Neubauer, F.  
562 (Eds.). Springer, pp. 567-583.

563 Schmid, R., Wood, B.J., 1976. Phase relationships in granulitic metapelites from the Ivrea-  
564 Verbano zone (Northern Italy). *Contributions to Mineralogy and Petrology* 54, 255-279.

565 Schmid, S.M., Zingg, A., Handy, M., 1987. The kinematics of movements along the Insubric  
566 Line and the emplacement of the Ivrea Zone. *Tectonophysics* 135, 47-66.

567 Sills, J.D., Tarney, J., 1984. Petrogenesis and tectonic significance of amphibolites  
568 interlayered with metasedimentary gneisses in the Ivrea Zone, Southern Alps, northwest  
569 Italy. *Tectonophysics* 107, 187-206.

570 Sinigoi, S., Quick, J.E., Clemens-Knott, D., Mayer, A., Demarchi, G., Mazzucchelli, M.,  
571 Nehrini, L., Rivalenti, G., 1994. Chemical evolution of a large mafic intrusion in the lower  
572 crust, Ivrea-Verbano Zone, northern Italy. *Journal of Geophysical Research* 99, 21,575-  
573 521,590.

574 Sinigoi, S., Quick, J.E., Mayer, A., Budahn, J., 1996. Influence of stretching and density  
575 contrasts on the chemical evolution of continental magmas: an example from the Ivrea-  
576 Verbano Zone. *Contributions to Mineralogy and Petrology* 123, 238-250.

577 Sinigoi, S., Quick, J.E., Demarchi, G., Kloetzli, U., 2011. The role of crustal fertility in the  
578 generation of large silicic magmatic systems triggered by intrusion of mantle magma in  
579 the deep crust. *Contributions to Mineralogy and Petrology* 162, 691-707.

580 Sun, S.s., McDonough, W.F., 1989. Chemical and isotopic systematics of oceanic basalts:  
581 implications for mantle composition and processes. Geological Society, London, Special  
582 Publications 42, 313-345.

583 Vavra, G., Schmid, R., Gebauer, D., 1999. Internal morphology, habit and U-Th-Pb  
584 microanalysis of amphibolite-to-granulite facies zircons: geochronology of the Ivrea Zone  
585 (Southern Alps). *Contributions to Mineralogy and Petrology* 134, 380-404.

586 White, R.W., 2008. Insights gained from the petrological modelling of migmatites: particular  
587 reference to mineral assemblages and common replacement textures. *Mineralogical*  
588 *Association of Canada, short course notes*, 38, 77–96.

589 White, R.W., Powell, R. 2002. Melt loss and the preservation of granulite facies mineral  
590 assemblages. *Journal of Metamorphic Geology* 20, 621–632.

591 White, R.W., Powell, R., Halpin, J.A., 2004. Spatially-focussed melt formation in aluminous  
592 metapelites from Broken Hill, Australia. *Journal of Metamorphic Geology*, 22, 825–845.



593 Wyllie, P.J., Wolf, M.B., 1993. Amphibolite dehydration-melting: sorting out the solidus.  
594 Geological Society, London, Special Publications 76, 405-416.

595 Zingg, A., 1978. Regionale Metamorphose in der Ivrea Zone (Nord-Italien). PhD thesis, ETH  
596 Zürich.

597 Zingg, A., 1980. Regional Metamorphism in the Ivrea Zone (Southern Alps, N-Italy): Field  
598 and microscopic Investigations. Schweizerische Mineralogische und Petrographische  
599 Mitteilungen 60, 153-179.

600

601 **Figure Captions**

602 **Fig. 1.** Simplified geological map of the central Ivrea Zone in the Southern Alps, Italy  
603 (compiled after Bigi et al., 1990; Rutter et al., 2007; Zingg, 1980). Mineral isograds after  
604 Schmid (1967) and Zingg (1980).

605  
606 **Fig. 2.** Schematic map of Val Strona di Omegna showing sample localities. Mineral isograds  
607 are based on the first macroscopic appearance of the appropriate mineral in the field (see also  
608 e.g., Redler et al., 2012; Schmid, 1967; Zingg, 1980).

609  
610 **Fig. 3.** Field relationships of metabasic rocks within the Kinzigite Formation in Val Strona di  
611 Omegna. **(a)** Typical fine-grained amphibolite with quartz vein from the mid amphibolite  
612 facies (sample IZ 014b; Loreglia). **(b)** Patch-migmatite close to the transition of the upper  
613 amphibolite to granulite facies. The leucosome forms irregular patches and large  
614 clinopyroxene porphyroblasts. **(c)** Stromatic migmatite foliation parallel leucosome (L1) and a  
615 discordant coarse-grained leucosome (L2) vein. The leucosomes mostly consist of plagioclase  
616 and quartz and contain peritectic clinopyroxene. **(d)** Metabasic granulite facies migmatite  
617 containing schlieren and schollen. The migmatite is dominated by melanosome (M)  
618 containing hornblende, clinopyroxene, orthopyroxene, garnet, biotite and minor plagioclase  
619 and quartz. The coarse-grained peritectic cpx-bearing leucosome occurs as network structures.  
620 **(e)** Metatexitic migmatite from the lowest granulite facies. The boudinaged melanosome (M)  
621 is surrounded by thin layers of fine-grained leucosome (L<sub>1</sub>). Coarse grained leucosome  
622 enriched in clinopyroxene (L<sub>2</sub>) forms pools within interboudin partitions. Above the boudin a  
623 coarse-grained leucocratic vein cross-cuts the rock (L<sub>3</sub>). **(f)** Granulite facies metabasic rock  
624 with garnet porphyroblasts. The garnet shows reaction coronae of plagioclase, hornblende and  
625 ilmenite. **(g)** Metabasic migmatite in which the leucosome (L) formed a network structure  
626 around the melanosome (M). **(h)** The upper and lower part of the photograph is dominated by

627 mesosomes consisting mostly of hornblende and clinopyroxene with minor plagioclase and  
628 quartz.  $L_1$  represents *in situ* leucosome formation in a pressure shadow of a fold. In source  
629 leucosome ( $L_2$ ) has pooled above clinopyroxene. The leucosome ( $L_3$ ) in the centre records  
630 migration of anatectic melt into veins. Below the leucosome vein residual material forms a  
631 mafic selvage dominated by hornblende. **(i)** Metabasic rock with typical migmatite texture in  
632 Campello Monti. The leucosome contains large peritectic clinopyroxene porphyroblasts. **(j)**  
633 Close up of the leucosome shown in (i). The leucosome is coarser grained than the  
634 melanosome and consists mostly of plagioclase with minor quartz & K-feldspar. Large  
635 clinopyroxene porphyroblasts in the leucosome are partially replaced by hornblende.

636

637 **Fig. 4.** Petrography of the metabasic rocks in Val Strona di Omegna (scale bar 1 mm). **(a)** Mid  
638 amphibolite facies sample containing lepidoblastic hornblende and biotite crystals. In some  
639 place the hornblende and biotite are intergrown while in other the hornblende is replaced by  
640 biotite. The biotite crystals define a foliation. **(b)** (crossed polars) Metabasic rock from the  
641 upper amphibolite facies (IZ 035) containing clinopyroxene in the matrix as well as  
642 porphyroblasts. The matrix minerals (clinopyroxene, plagioclase and hornblende) are general  
643 relative equigranular however in some areas (white rectangular) the crystals become coarser  
644 grained and often show  $120^\circ$  angle between mineral grains. **(c)** Granulite facies sample with  
645 the mineral assemblage clinopyroxene, orthopyroxene, garnet, brown hornblende, plagioclase,  
646 ilmenite and secondary biotite. Most mineral grains show triple junctions with an angle of  
647  $120^\circ$ . **(d)** Highest grade sample (IZ 100, Campello Monti, see Fig. 2) from the granulite facies  
648 containing the peak mineral assemblage clinopyroxene, orthopyroxene, garnet, plagioclase  
649 and ilmenite. Brown hornblende and biotite in this sample are only present as secondary  
650 replacements. **(e)** Granulite facies migmatite with leucosome and melanosome domains. The  
651 area from the left to the middle is dominated by quartz and plagioclase with minor  
652 clinopyroxene (leucosome). The upper right corner is enriched in clinopyroxene, hornblende,

653 orthopyroxene, biotite and ilmenite with only minor plagioclase and quartz (melanosome).  
654 The grain size in the leucosome domain is in general larger than in the melanosome domain.  
655 **(f)** (crossed polars) Leucosome vein with large plagioclase and quartz grains compared to  
656 'normal' granulite facies grain sizes (right side). The leucosome is bordered by a mafic  
657 selvages enriched in brown, hornblende. **(g)** Garnet reaction corona (Fig. 3f). The garnet is  
658 rimmed by plagioclase, ilmenite and brown hornblende. **(h)** Retrograde replacement of high-  
659 grade mineral assemblages occurs in several steps. Clinopyroxene gets replaced by brown  
660 hornblende, which then is replaced by biotite (white arrows) and/or actinolite.

661

662 **Fig. 5.** Harker variation diagrams showing the concentrations of major elements (wt%) in  
663 metabasic rocks from Val Strona di Omegna. Average values of the middle and lower  
664 continental crust are taken from Rudnick and Gao (2003).

665

666 **Fig. 6. (a–c)** Trace element composition of metabasic rocks from Val Strona di Omegna  
667 normalised to primitive mantle (McDonough and Sun, 1995). The values for N-MORB  
668 (Hofmann, 1988; Sun and McDonough, 1989) and E-MORB (Sun and McDonough, 1989)  
669 and the middle and lower continental crust (Rudnick and Gao, 2003) are shown. **(d)**  
670 Comparison of trace elements content of mafic rocks (amphibole gabbros & norites) from the  
671 Mafic Complex, Val Sessera (Sinigoi et al., 2011) with metabasic rocks (this study) from the  
672 Kinzigite Formation in Val Strona di Omegna (Campello Monti).

673

674 **Fig. 7. (a–c)** REE composition of metabasic rocks from Val Strona di Omegna normalised to  
675 CI Chondrite (McDonough and Sun 1995). The values for N-MORB and E-MORB are from  
676 Hofmann (1988) and Sun and McDonough (1989), for the middle and lower continental crust,  
677 Rudnick and Gao (2003). **(d)** Comparison of REE content of mafic rocks (amphibole gabbros

678 & norites) from the Mafic Complex, Val Sessera (Sinigoi et al., 2011) with metabasic rocks  
679 (this study) from the Kinzigite Formation in Val Strona di Omegna (Campello Monti).

680

681 **Fig. 8.** Diagrams showing average major **(a)**, trace **(b)** and rare earth **(c)** element composition  
682 of the upper amphibolite and granulite facies normalised to the average mid amphibolite  
683 facies composition. **(a)** The average major elements composition of the upper amphibolite and  
684 granulite facies show a depletion in  $\text{SiO}_2$ ,  $\text{Al}_2\text{O}_3$ ,  $\text{Na}_2\text{O}$  and  $\text{K}_2\text{O}$  compared to average mid  
685 amphibolite samples, whereas  $\text{TiO}_2$ ,  $\text{FeO}$ ,  $\text{MnO}$ ,  $\text{MgO}$  and  $\text{CaO}$  are enriched. **(b)** The trace  
686 elements of the upper amphibolite and granulite facies are depleted in LILE. The HFSE show  
687 values similar to average mid amphibolite facies samples. **(c)** The LREE are depleted in the  
688 upper amphibolite facies while the granulites show values close to average mid amphibolite  
689 facies concentration. The average upper amphibolite and granulite facies compositions show a  
690 slightly HREE enrichment compared to mid amphibolite facies samples.

691

692 **Table Captions**

693

694 **Table 1.** Major mineral assemblages of representative metabasic rocks from Val Strona di

695 Omegna.

696

697 **Table 2.** Whole rock major and trace element composition of representative metabasic rocks

698 from Val Strona di Omegna. Iron contents are expressed as all ferric. Trace elements marked

699 with an asterisk were measured by XRF, all other by LA-ICP-MS.

Figure1

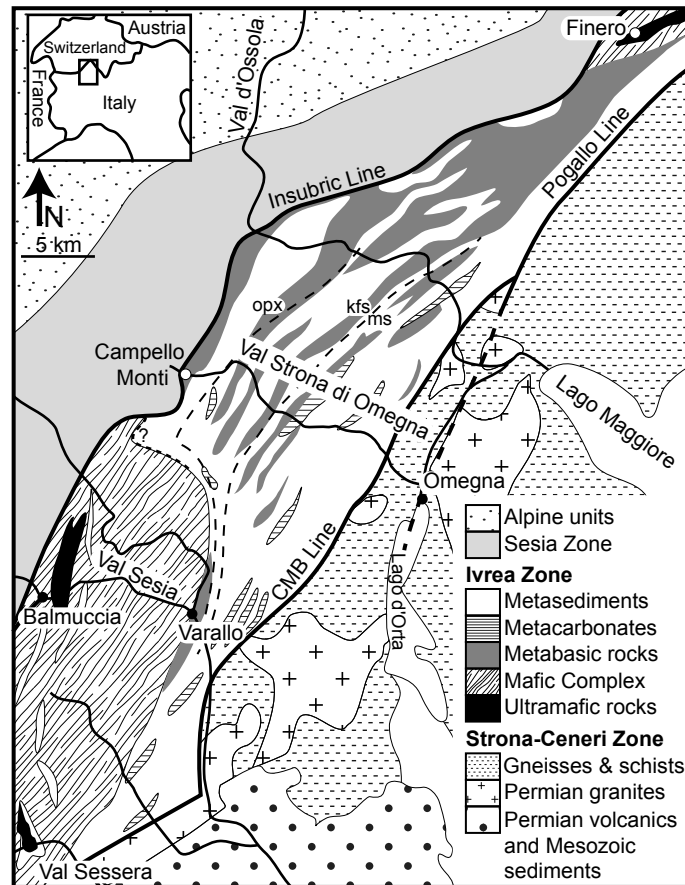


Figure2

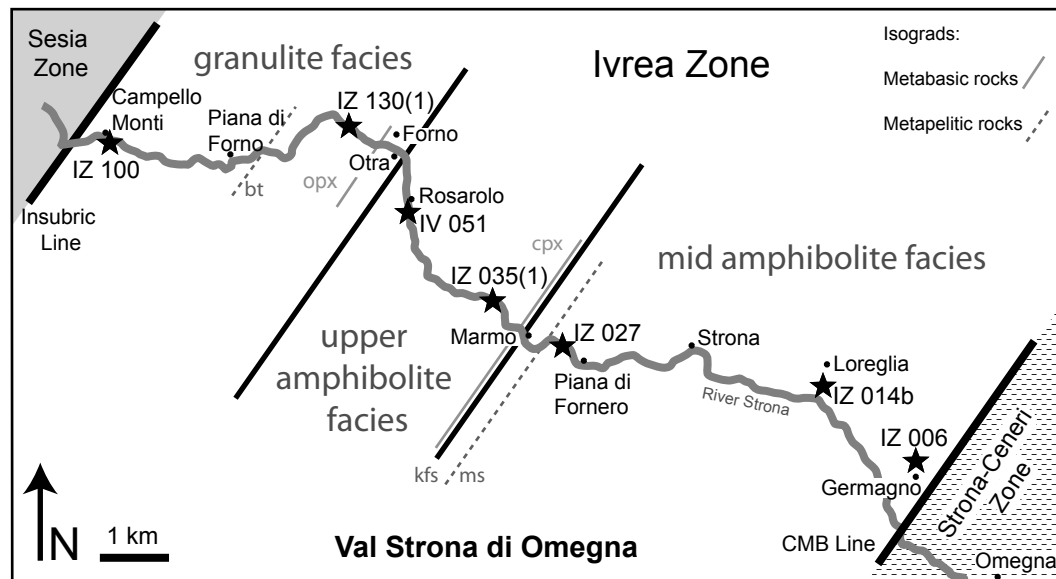




Figure3 Part1  
[Click here to download high resolution image](#)

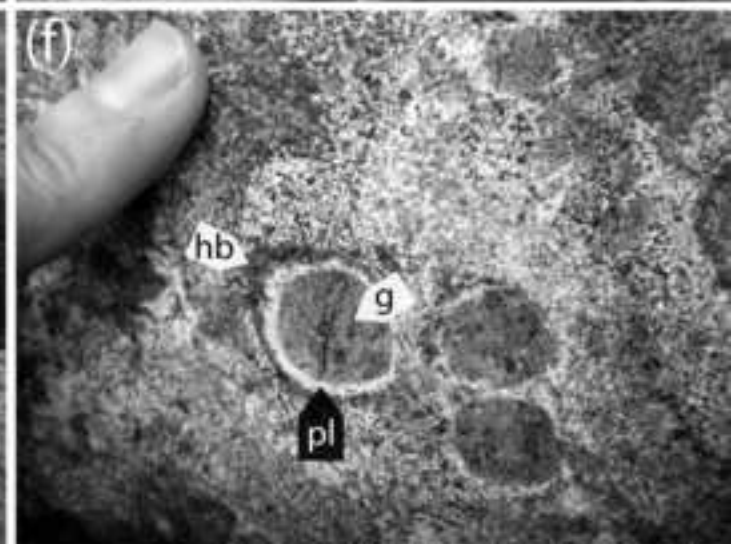
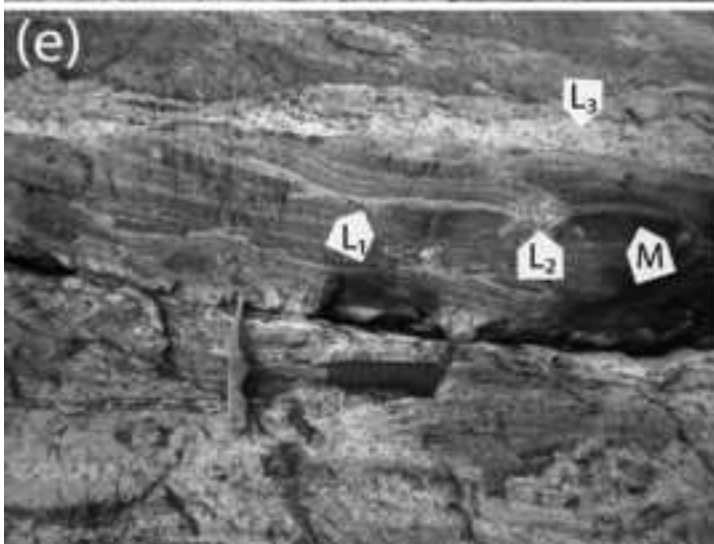
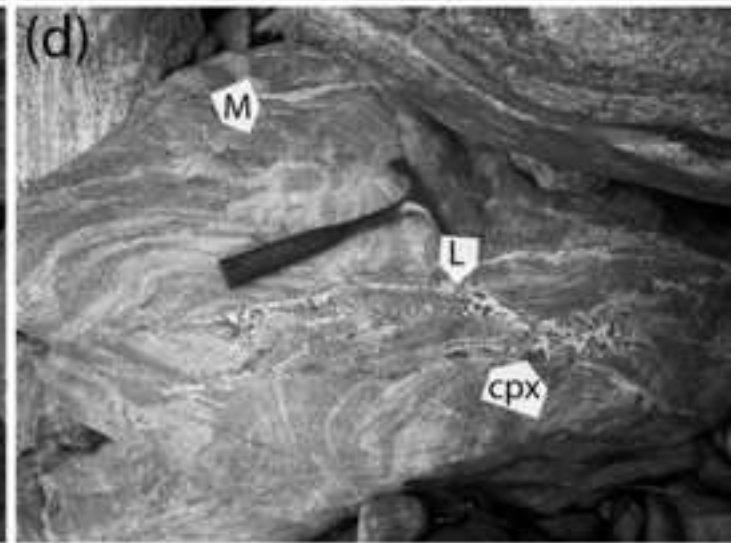
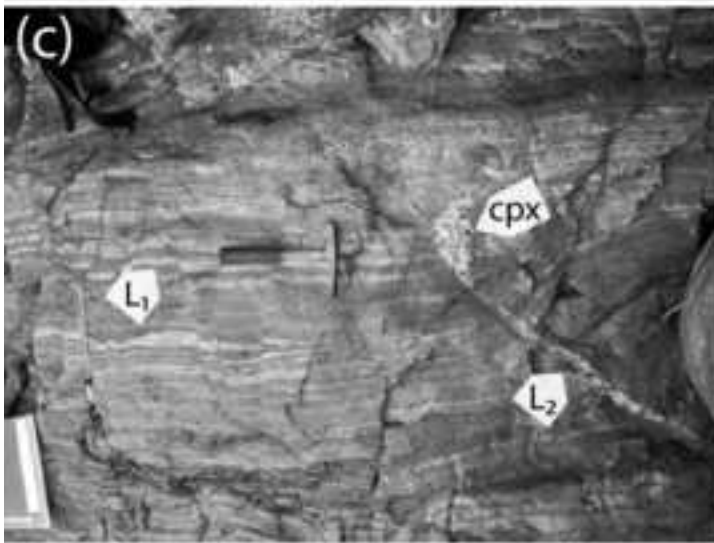
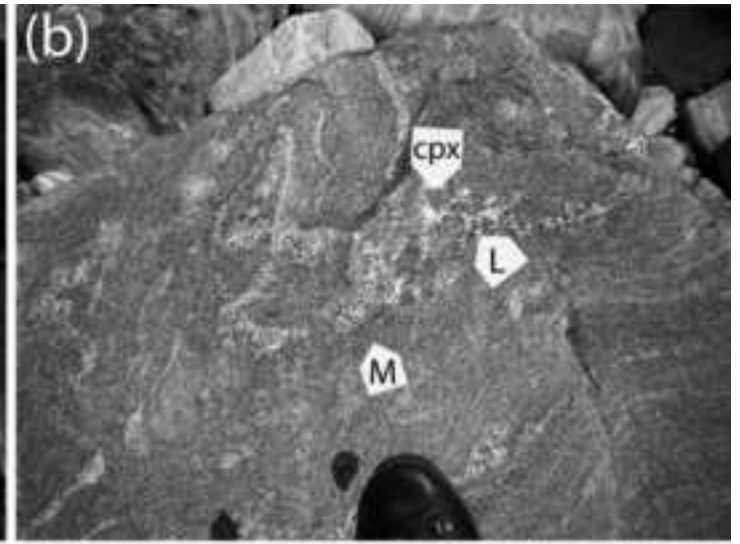


Figure 3 Part2  
[Click here to download high resolution image](#)

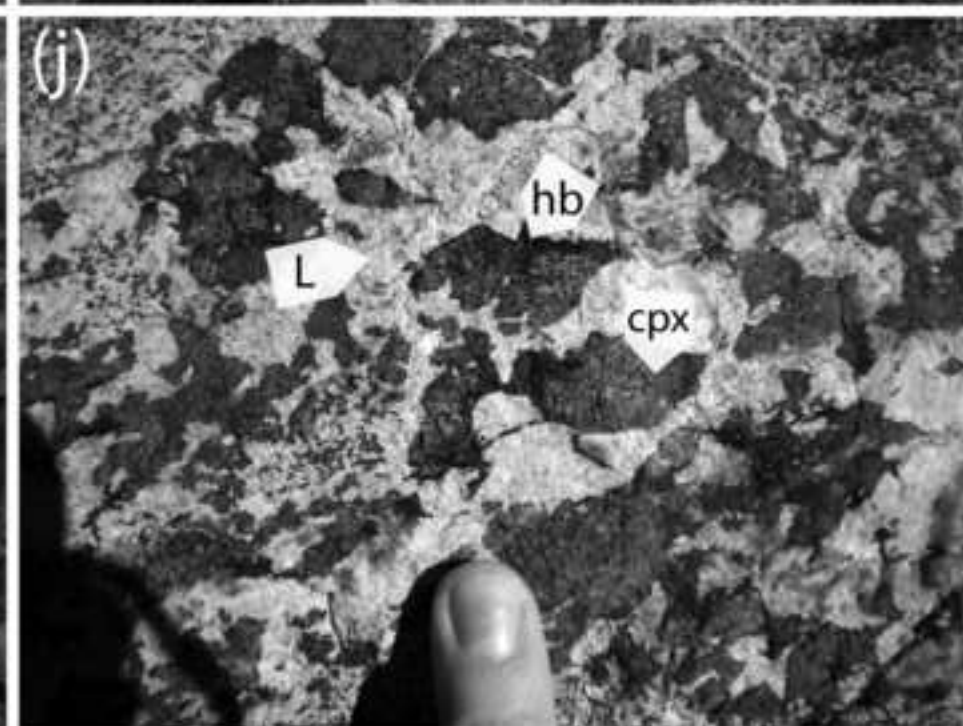
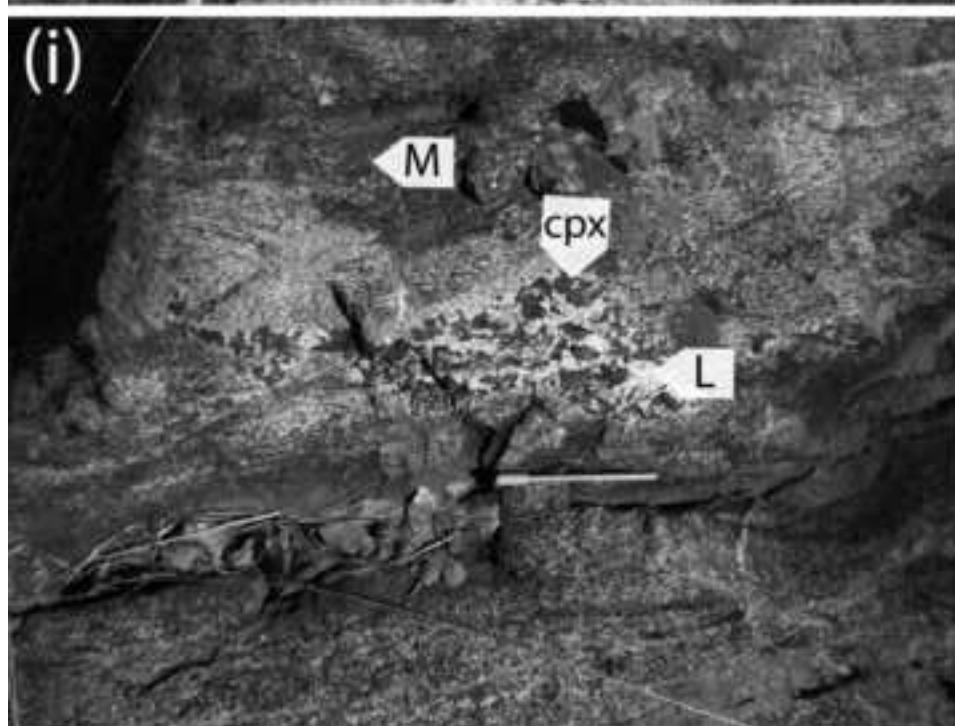
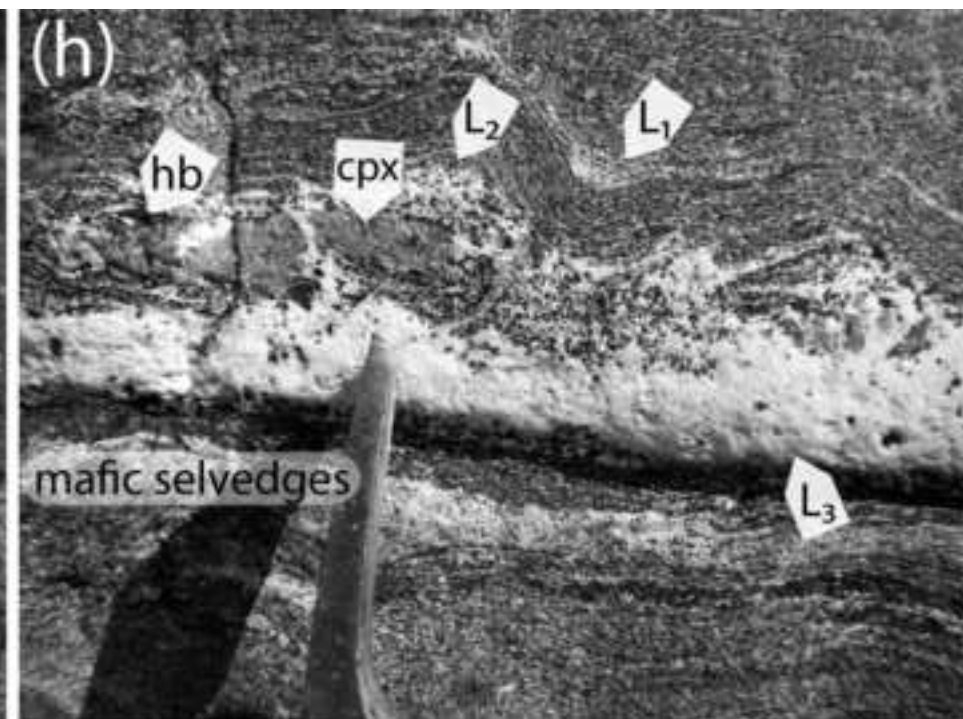
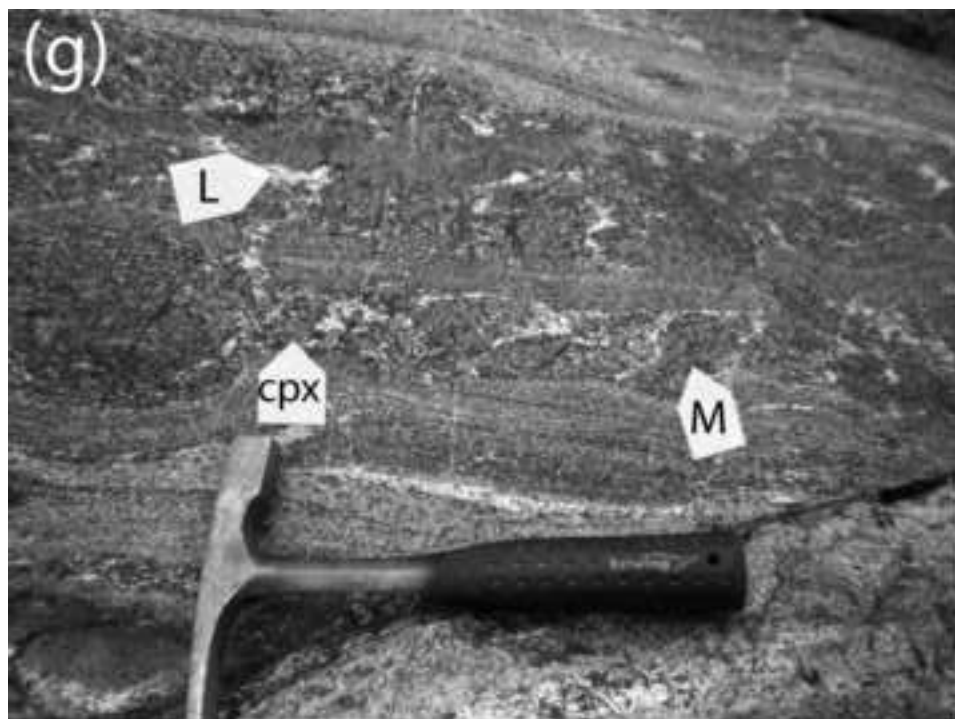


Figure4  
[Click here to download high resolution image](#)

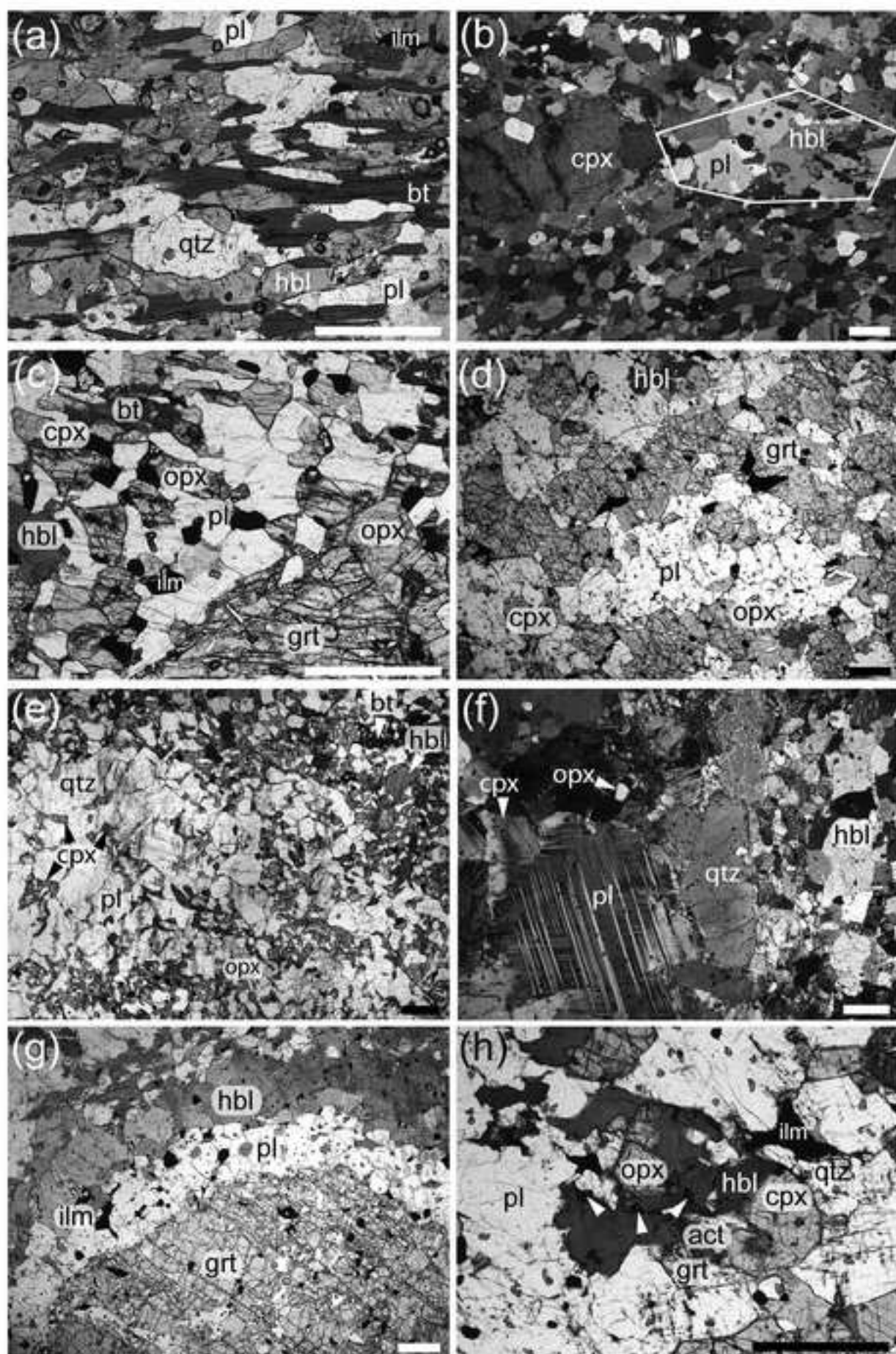


Figure 5

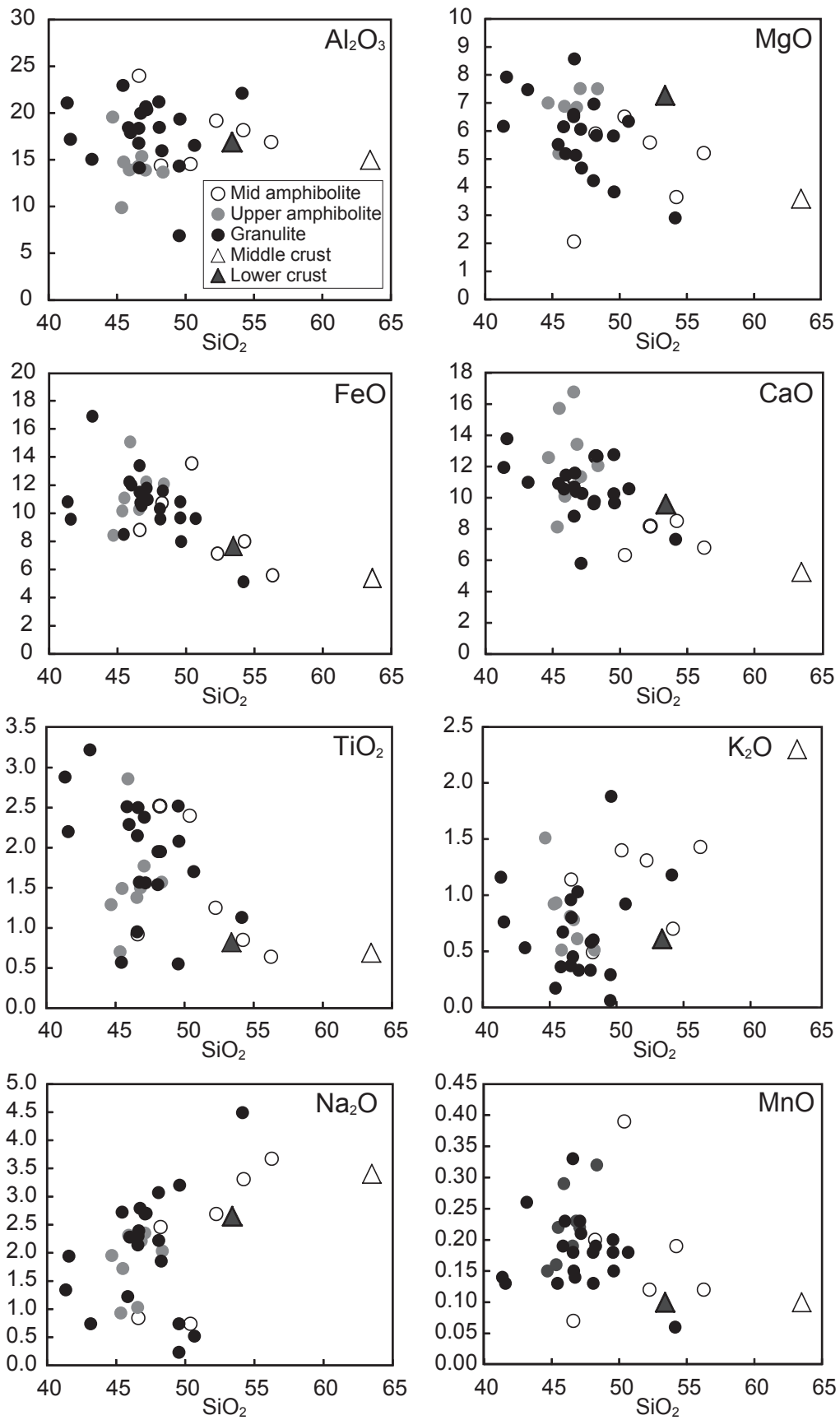


Figure6

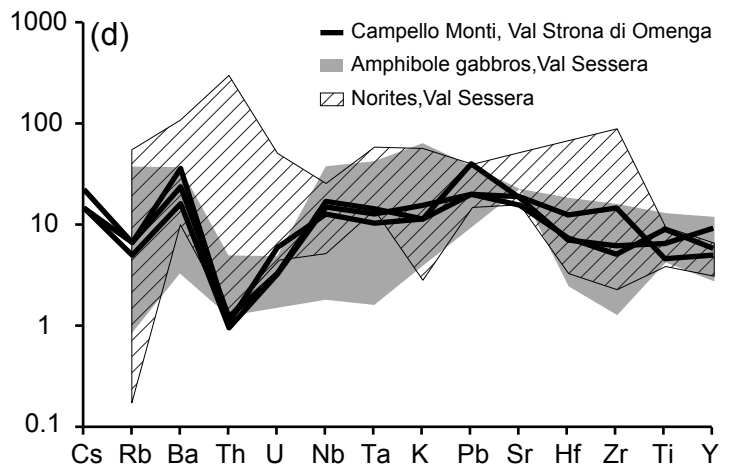
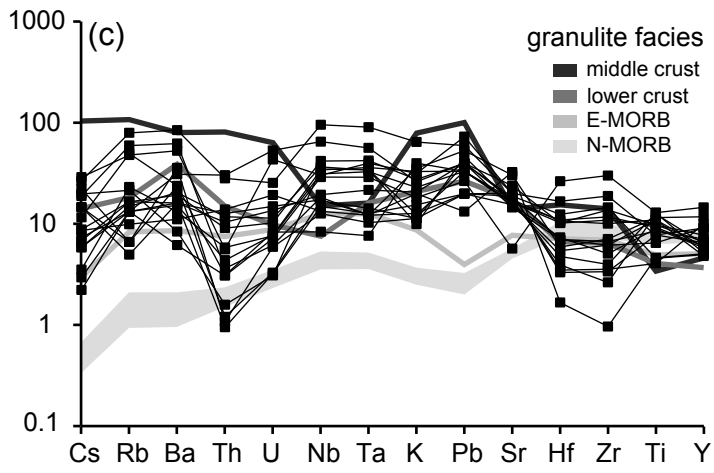
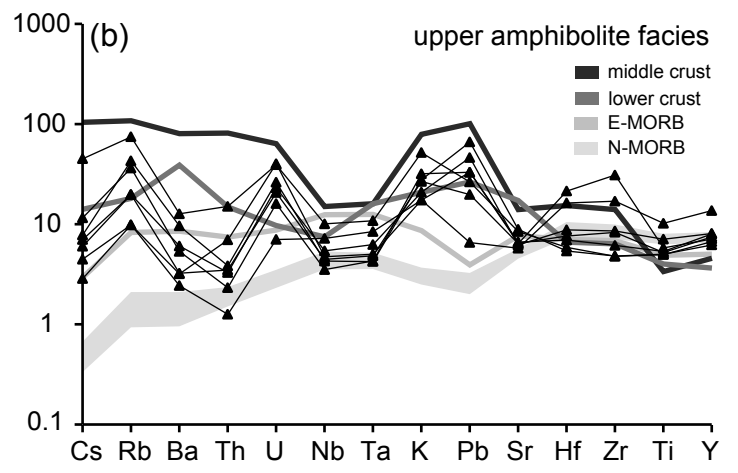
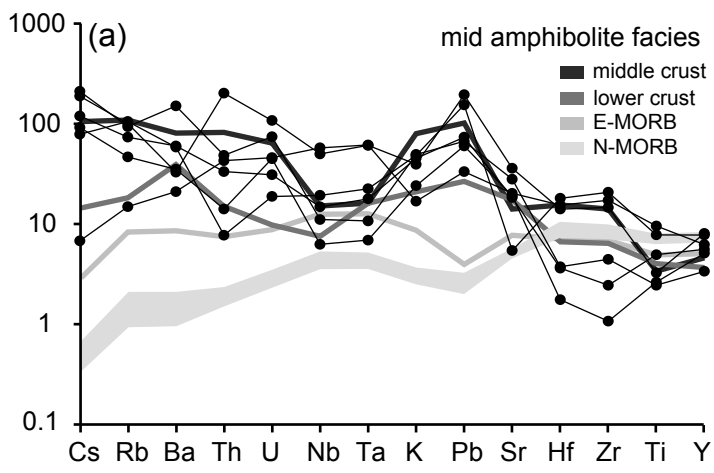


Figure 7

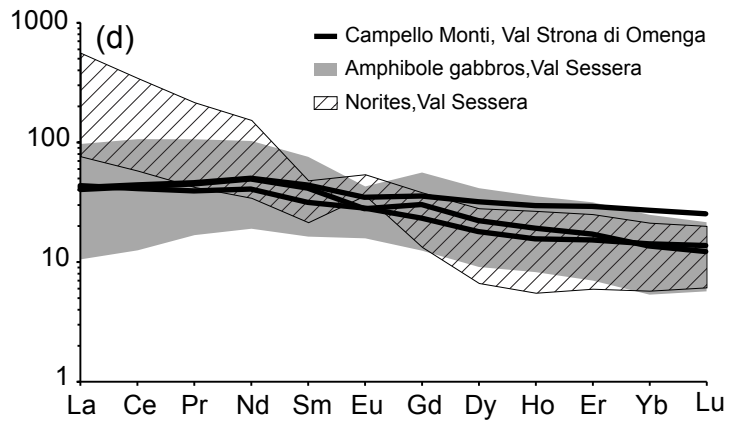
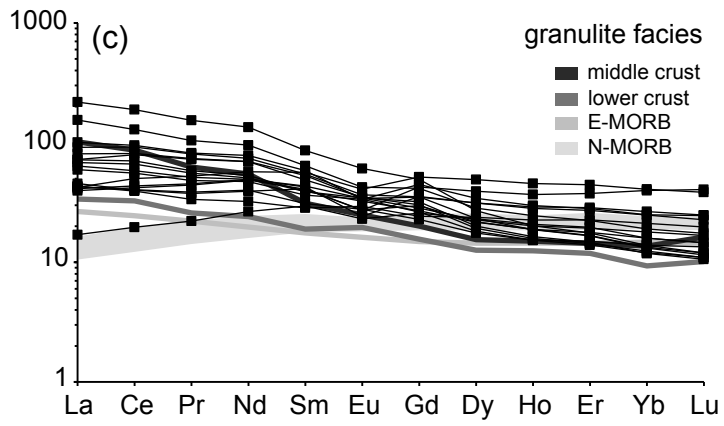
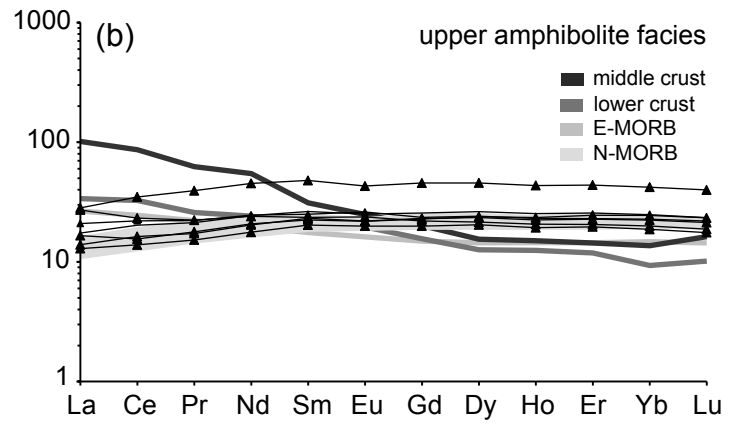
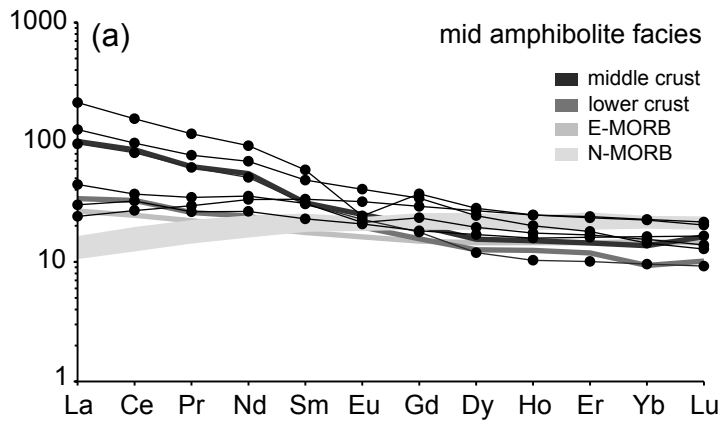


Figure 8

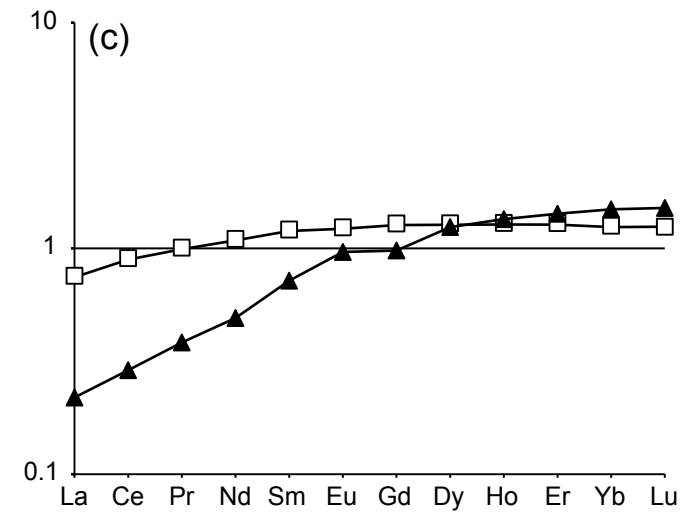
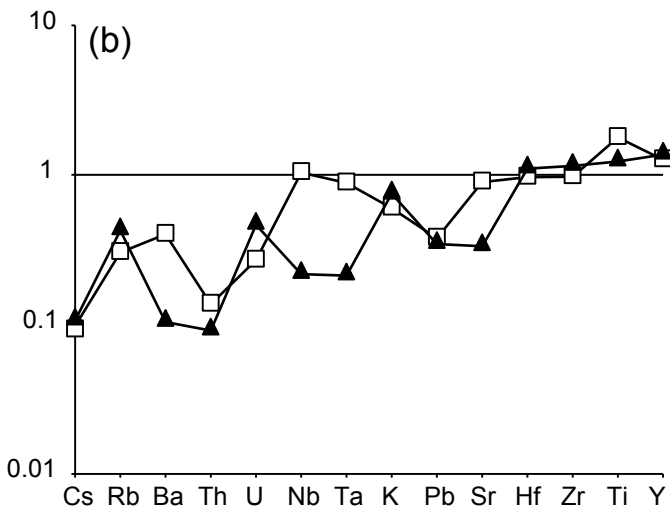
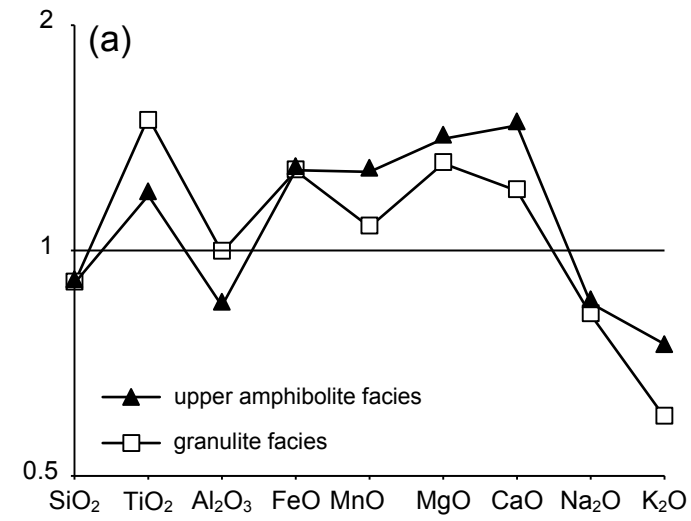






Table2

[Click here to download Table: Tab2.pdf](#)

<b>Sample</b>	<b>IZ 006</b>	<b>IZ 014b</b>	<b>IZ 027</b>	<b>IZ 035(1)</b>	<b>IV 051</b>	<b>IZ 130(1)</b>	<b>IZ 161(1)</b>	<b>IZ 100</b>
<i>Major elements (wt%)</i>								
<b>SiO<sub>2</sub></b>	54.22	52.25	50.37	48.35	45.90	48.27	45.99	47.17
<b>TiO<sub>2</sub></b>	0.85	1.25	2.40	1.57	2.86	1.95	2.29	1.56
<b>Al<sub>2</sub>O<sub>3</sub></b>	18.16	19.18	14.53	13.68	13.91	15.96	17.90	20.35
<b>Fe(total)</b>	8.94	7.95	15.13	13.49	16.84	12.95	13.41	12.26
<b>MnO</b>	0.19	0.12	0.39	0.32	0.29	0.19	0.23	0.21
<b>MgO</b>	3.64	5.59	6.51	7.50	6.88	5.84	5.19	4.68
<b>CaO</b>	8.51	8.18	6.33	12.05	10.09	12.66	11.44	10.27
<b>Na<sub>2</sub>O</b>	3.31	2.69	0.74	2.03	2.31	1.85	2.28	2.70
<b>K<sub>2</sub>O</b>	0.70	1.31	1.40	0.51	0.51	0.60	0.67	0.33
<b>P<sub>2</sub>O<sub>5</sub></b>	0.19	0.10	0.23	0.12	0.26	0.17	0.29	0.30
<b>SO<sub>3</sub></b>	0.02	-0.01	0.36	0.02	0.00	0.03	1.37	0.05
<b>Sum</b>	99.60	99.99	101.00	100.09	100.21	100.54	101.61	99.96
<b>LOI</b>	0.86	1.36	2.57	0.41	0.35	0.02	0.51	0.07
<i>Trace elements (ppm)</i>								
<b>Li</b>	40.34	21.61	39.49	11.85	9.31	6.59	6.85	3.35
<b>Sc*</b>	31.00	32.00	44.00	50.00	54.00	43.00	45.00	40.00
<b>Ti</b>	3212.31	6018.29	9477.04	6391.21	12466.21	10283.52	11856.28	7866.95
<b>V</b>	239.90	307.45	379.38	305.69	457.12	256.56	290.30	226.45
<b>Cr*</b>	25.00	16.00	98.00	179.00	63.00	177.00	112.00	18.00
<b>Mn</b>	1419.20	915.03	2692.72	2085.01	1967.21	1243.41	1616.68	1478.14
<b>Ni*</b>	14.00	8.00	58.00	68.00	57.00	66.00	61.00	18.00
<b>Rb*</b>	28.00	44.00	63.00	6.00	6.00	10.00	14.00	4.00
<b>Sr</b>	381.20	366.64	109.35	130.47	116.42	290.86	327.13	367.15
<b>Y</b>	22.22	24.25	33.68	32.64	59.53	30.76	28.78	39.76
<b>Zr</b>	11.47	26.10	218.57	88.46	180.32	70.90	144.92	65.18
<b>Nb</b>	4.17	9.81	12.77	3.17	4.82	12.88	20.69	11.19
<b>Cs</b>	1.92	2.50	1.65	0.10	0.06	0.19	0.07	0.31
<b>Ba</b>	232.24	395.74	385.66	21.47	16.40	107.23	87.42	156.67
<b>La</b>	7.10	10.50	5.68	4.95	6.67	10.33	16.26	9.83
<b>Ce</b>	19.76	22.59	16.45	13.47	21.32	24.30	40.77	26.75
<b>Pr</b>	2.43	3.21	2.73	2.05	3.64	3.13	5.19	4.22
<b>Nd</b>	12.06	16.18	15.17	11.21	20.63	14.83	23.31	22.69
<b>Sm</b>	3.38	4.56	4.94	3.69	7.07	4.24	5.79	6.44
<b>Eu</b>	1.17	1.20	1.79	1.47	2.42	1.66	1.95	1.93
<b>Gd</b>	3.62	4.65	5.79	4.67	9.06	4.86	5.67	7.01
<b>Dy</b>	4.16	4.78	6.59	5.91	11.20	5.88	5.60	7.75
<b>Ho</b>	0.86	0.95	1.34	1.26	2.37	1.24	1.10	1.60
<b>Er</b>	2.57	2.68	3.82	3.67	7.00	3.64	3.10	4.60
<b>Yb</b>	2.62	2.48	3.64	3.65	6.76	3.43	2.91	4.30
<b>Lu</b>	0.40	0.34	0.53	0.54	0.98	0.49	0.41	0.61
<b>Hf</b>	0.51	1.04	5.13	2.19	4.67	1.99	2.92	2.00
<b>Ta</b>	0.26	0.66	0.83	0.19	0.32	0.81	1.22	0.53
<b>Pb*</b>	9.00	11.00	23.00	5.00	1.00	6.00	5.00	6.00
<b>Th</b>	1.13	2.66	0.62	0.56	0.10	0.83	0.47	0.10
<b>U</b>	0.91	0.63	0.38	0.82	0.15	0.28	0.16	0.07